New Geometric Constraints in Slider ABS Optimization

Hong Zhu and David B. Bogy

Computer Mechanics Laboratory

Department of Mechanical Engineering

University of California at Berkeley

Berkeley, CA 94720

ABSTRACT

This report addresses new geometric constraints, in which we define not only constraint points, but also constraint rails and constraint lines. Then we apply these geometric constraints to slider ABS optimization problems. The new geometric constraints make the slider ABS optimization much easier by enabling users to explore a much wider range of constraints in practical ABS optimization problems. We also discuss the issue of slider ABS sensitivity optimization and propose the basic idea of how to perform the sensitivity optimization. Some possible ways to improve the efficiency for the sensitivity optimization are also proposed.

1. INTRODUCTION

In the previous CML air bearing surface design optimization program (version 1.5 developed by O'Hara (1997)), the only geometric constraints defined in each optimization problem were the constraint points themselves. This meant that, for instance, we could only alter the points defining the rails to move in the length or width directions within certain intervals. As designs have gotten more complex the need for greater flexibility in constraint definition has arisen. For example, if an entire rail needed to be rotated in order to find the optimized ABS design, it could not be done by such a limitation on constraints. Therefore, in order to extend the capability of the optimization program, we need to introduce some new geometric constraints.

In this report, we first introduce the definition of the new geometric constraints, and then we apply them to slider ABS optimization. We also discuss the concept of slider ABS design sensitivity optimization.

2. DEFINITION OF NEW GEOMETRIC CONSTRAINTS

Figure 1 shows a comparison between the new geometric constraints and the old geometric constraints. In the new geometric constraints, we not only define constraint points, we also define constraint rails and constraint lines. The constraint rails can be translated in either the length or width direction, rotated with respect to a fixed point, and expanded or

shrunk proportionally. The constraint lines can be translated in either the length or width direction, rotated with respect to a fixed point, and extended or contracted along the length direction. To maintain a symmetrical slider ABS design and fixed local geometric shapes, we also define symmetrical and relative constraints for constraint rails and constraint lines. Please refer to CML technical report "The CML Air Bearing Optimization Program Version 3.0" for more details.

We demonstrate the new rail constraints in Figs. 2 ~ 4. In these figures, the gray lines show the original slider ABS design, and the dark lines show the shape of the slider ABS design after the rail deformation. Notice that we also define symmetrical constraints in order to maintain a symmetrical slider ABS design. In Fig. 2, a rear rail is translated in the length direction. In Fig. 3, a rear rail is rotated with respect to one of its rail points. In Fig. 4, a front rail is shrunk proportionally.

We demonstrate the new line constraints in Figs. 5 ~ 7. In these figures, the gray lines show the original slider ABS design, and the dark lines show the shape of the slider ABS design after the line deformation. We also define symmetrical constraints in order to maintain a symmetrical slider ABS design. In Fig. 5, a line is translated in the length direction. In Fig. 6, a line is rotated with respect to one of its endpoints. In Fig. 7, a line is extended along its length direction.

Next we apply those new geometric constraints to slider ABS optimization problems.

3. APPLICATION TO SLIDER ABS OPTIMIZATION

3.1 Air bearing design optimization problems

The optimization problem defined here is: given a prototype slider ABS design, optimize it to obtain uniform flying heights near the target flying height and a flat roll profile across the disk.

To demonstrate the application of the new geometric constraints, we use a so-called "Enterprise" slider as the prototype slider. This is a Pico slider that flies over a disk rotating at 7200 RPM with FHs around 5nm. Its rail shape and its 3-dimensional rail geometry are shown in Figs. 8 and 9, respectively.

We wish to lower the flying heights of this slider to the target flying height (i.e., 3.5nm), and at the same time maintain a flat roll profile at the three different radial positions OD, MD and ID. The objective function or cost function is defined as:

$$\begin{aligned} &\boldsymbol{1}\times(\textit{FH Max Difference term}) + \boldsymbol{9}\times(\textit{FH term}) + \boldsymbol{1}\times(\textit{Roll term}) + \\ &\boldsymbol{1}\times(\textit{Roll Cutoff term}) + \boldsymbol{0}\times(\textit{Pitch Cutoff term}) + \boldsymbol{0}\times(\textit{Vertical Sensitivity term}) + \\ &\boldsymbol{0}\times(\textit{Pitch Sensitivity term}) + \boldsymbol{0}\times(\textit{Roll Sensitivity term}) + \boldsymbol{0}\times(\textit{Negative Force term}) . \end{aligned}$$

Note that since we are primarily concerned with the flying heights, we put a heavier weight (9) on that term. Because our only objective is to lower the FHs and maintain a flat roll profile, we put a 0 weight on all the sensitivity terms and the negative force term.

We did not define a manufacturing tolerance, but we did impose the hidden constraints:

FH ≤ 2 nm or FH ≥ 10 nm or Roll ≤ -30 μrad or Roll ≥ 30 μrad.

3.2 Air bearing design optimization results

For the same prototype slider ABS design, the same objective function and the same hidden constraints, we carried out optimizations for two cases: a 4-D case and a 2-D case.

3.2.1 4-D ABS optimization results

For the 4-D ABS optimization case, we defined four original constraint rails. The front rail and the rear rail can be expanded or shrunk. The side rails can be expanded or shrunk and also translated in the length direction and. Figure 10 shows the four original constraint rails. Notice that we also defined constraints to maintain the symmetrical configuration of the "Enterprise" slider design.

Figure 11 shows the variation of the objective function value during the optimization process. It shows that, although we defined relatively "loose" hidden constraints, there are still many infeasible samples. We see that there are 160 infeasible samples (N_{ign}) out of the 224 samples generated. This means that the design is quite sensitive to some of the constraint

rails, i.e., small changes may have large effects on the slider performance. The objective function value was lowered from the initial value 11 to the final value of 2.455.

Figure 12 shows the comparison between the initial design and the optimized design. The gray lines represent the initial "Enterprise" design and the dark lines represent the final optimized design. From Fig. 12 we see that for the optimized design, the front rail and the rear rail remain unchanged. Only the side rails have been shrunk and moved toward the leading edge.

Figure 13 shows the variations of the slider's performance parameters for all the best-so-far ABS designs found during the optimization process. Table 1 summarizes the optimization results by comparing the FHs, Rolls and Pitches of the initial and the optimized designs. We observe that the optimized ABS design has uniform FHs around the 3.5nm target and maintains a flat roll profile.

3.2.2 2-D ABS optimization results

In optimization care must be taken to define the constraints properly. Improperly defined constraints might yield only slightly optimized results or even no optimization at all. We also want to keep the dimensions of an optimization problem as low as possible, because lower dimensions mean a smaller search space, and a smaller search space means the optimized design is found more rapidly.

The previous 4-D ABS optimization results show that in order to lower the FHs of the "Enterprise" slider from 5nm to 3.5nm, we need only change the shape and location of the side rails. Therefore, in our next example we define only two original constraints for the side rails, i.e., they can be moved in the length direction and expanded or shrunk. The front rail and the rear rail remain fixed in this case.

Figure 14 shows the variation of the objective function value during the optimization process. After we removed the two constraints for the front rail and the rear rail, which are quite sensitive, the number of infeasible sample points has been reduced substantially. In this case there are only 18 infeasible samples out of the 401 samples generated. The objective function value has been lowered from the initial value of 11 to the final value of 1.809, which is smaller than the value of 2.455 in the 4-D case. This indicates that the 2-D case found a better-optimized slider ABS design than did the previous 4-D case.

Figure 15 shows the comparison between the initial design and the optimized design. If we compare Fig. 15 with Fig. 12, we see that for the better-optimized ABS design found in the 2-D case, the side rails have been shrunk less than in the 4-D case, but they have been moved further toward the leading edge.

Figure 16 shows the variations of the slider performance parameters for all the best-so-far ABS designs found during the optimization process. Figure 17 shows the variations of the objective function terms for all the best-so-far designs. We see that the second objective function term, on which we put a heavier weight, has been reduced very effectively. Table 2

summarizes the optimization results by comparing the FHs, Rolls and Pitches of the initial and the optimized designs. If we compare Table 2 with Table 1, we see that the optimized ABS design found in the 2-D case has more uniform FHs around the 3.5nm target FH and that it also maintains a slightly flatter roll profile.

Figure 18 shows the distribution of the sample points within the search space for the 2-D slider ABS optimization case. Figure 19 shows a local zoom-in around the best point. The small dots in these two figures represent the sample points generated by the algorithm; the shadowed boxes represent the boxes containing the infeasible points; and the circular dot represents the best point found by the algorithm. The scatter pattern of the infeasible points inside the search space reflects to some extent the strong nonlinear property of this slider ABS optimization problem. Figure 20 shows the objective function contour lines according to the results obtained. The round dots represent the best-so-far sample points found by the algorithm during the optimization process.

4. SLIDER ABS SENSITIVITY OPTIMIZATION

One of the important issues of slider design and optimization is the slider ABS design sensitivity. Due to the manufacturing tolerance, there are always minor differences between the actual fabricated slider designs and the numerically optimized ones.

If the optimized slider ABS design is too sensitive for the manufacturing tolerance, that is, if minor manufacturing tolerance differences have large effects on the slider's

performance, then this optimized design will be unsuitable for fabrication. With high sensitivity, a large fraction of the fabricated sliders will fail to satisfy the performance requirements. Therefore, slider ABS sensitivity optimization is of great importance. In this report, we present only some preliminary thoughts on how to perform slider ABS sensitivity optimization. To carry out slider ABS sensitivity optimization, we need to include a sensitivity term in the objective function. That sensitivity term should involve slider performance parameters such as FHs, Rolls and Pitches. We also need to prescribe the sensitivity constraints. With use of the new geometric constraints, the definition of the sensitivity constraints becomes much easier. After each new sample ABS design is generated and evaluated, it is perturbed with the manufacturing tolerance according to the sensitivity constraints prescribed. After a set of perturbed ABS designs are generated and evaluated, the objective function is calculated. The optimization process continues. Figure 21 presents a schematic illustration for this process. The symbol Δ represents the manufacturing tolerance. We see that the new objective function consists of two parts: the first part contains the current objective function terms, and the second part is the sensitivity term.

As can be observed from Fig. 21, for every sample ABS design generated, at least two perturbed samples must be evaluated ($\pm\Delta$). For example, if we define two sensitivity constraints, for every new sample ABS design generated, four perturbed sample designs need to be evaluated to get the value of the sensitivity term. It follows that sensitivity optimization requires much longer simulation time. So naturally, we should also think of ways to improve the efficiency of sensitivity optimization. We propose two ways here to improve the efficiency when performing sensitivity optimization.

The first one is to make use of the hidden constraints during the sensitivity optimization. There are two cases. The first case is shown in Fig. 22. The idea is, if the sample design generated satisfies the hidden constraints and is identified as an infeasible design, then it will not be perturbed and the sensitivity term will not be evaluated. The second case is shown in Fig. 23. The idea is, if any of the perturbed designs satisfies the hidden constraints, the rest of the perturbed designs will not be generated and evaluated. Again the sensitivity term will not be evaluated. The sample design will be marked as infeasible and later it will be given a pseudo value.

The second way is to make use of the first part of the objective function, as shown in Fig. 24. The idea is, after we have evaluated the sample design generated and thus attained the value of the first part of the objective function, if that value is larger (by a weight ≥ 1) than the value of the objective function of the best-so-far optimized design, then we will not perturb it. The reason is obvious: that sample design will not become an optimized design because even if its sensitivity term is 0 its objective function value is still higher than that of the best-so-far optimized design.

The two methods we proposed here are expected to improve the efficiency of the sensitivity optimization by greatly reducing the slider ABS samples need to be evaluated.

5. CONCLUSION

In this report we defined new geometric constraints for slider ABS optimization, including not only constraint points, but also constraint rails and constraint lines.

The constraint rails can be translated in either the length or width direction, rotated with respect to a fixed point and expanded or shrunk proportionally. The constraint lines can be translated in either the length or width direction, rotated with respect to a fixed point and extended or contracted along its length direction. To maintain a symmetrical slider ABS design and fixed local geometric shapes, we also define symmetrical and relative constraints for the constraint rails and constraint lines.

We applied the new geometric constraints to slider ABS optimization problems, investigating a 4-D case and a 2-D case. Although we found satisfactory optimization results in both cases, a better-optimized slider ABS design was found in the 2-D case by redefining the constraints. This verifies the importance of properly defining constraints.

In conclusion, the new geometric constraints make the slider ABS optimization much easier by enabling users to explore a much wider range of constraints among those found in practical ABS optimization problems.

We also discussed the issue of the slider ABS sensitivity optimization. The definition of the new geometric constraints makes the sensitivity optimization much easier. We presented the basic idea for performing the sensitivity optimization. Some possible ways to improve the efficiency for the sensitivity optimization were also proposed.

ACKNOWLEDGEMENT

This study is supported by the Computer Mechanics Laboratory (CML) at the University of California at Berkeley and partially supported by the Extremely High Density Recordings (EHDR) project of the National Storage Industry Consortium (NSIC).

REFERENCES

1. Zhu, H. and Bogy, D., 2000, "Optimization of Slider Air Bearing Shapes using Variations of Simulated Annealing", Technical Report 00-010, Computer Mechanics Laboratory, University of California at Berkeley.

2. Zhu, H. and Bogy, D., 2001, "DIRECT Algorithm and its Application to Slider Air Bearing Surfaces Optimization", Technical Report 01-003, Computer Mechanics Laboratory, University of California at Berkeley.

3. Zhu, H. and Bogy, D., 2001, "Locally Biased Variations of the DIRECT Algorithm and their application to the Slider Air Bearing Surfaces Optimization", Technical Report 01-007, Computer Mechanics Laboratory, University of California at Berkeley.

4. Zhu, H. and Bogy, D., 2001, "Modifications to the DIRECT Algorithm", Technical Report 01-013, Computer Mechanics Laboratory, University of California at Berkeley.

5. Zhu, H. and Bogy, D., 2001, "The CML Air Bearing Optimization Program Version 2.0", Technical Report 01-016, Computer Mechanics Laboratory, University of California at Berkeley.

6. Zhu, H. and Bogy, D., 2002, "DIRECT Algorithm and Its Application To Slider Air Bearing Surface Optimization", *Intermag 2002 Conference*, Amsterdam, The Netherlands.

7. Zhu, H. and Bogy, D., 2002, "Hard disk drive air bearing design: Modified DIRECT algorithm and its application to slider Air Bearing Surface optimization", abstract accepted by *6th International Tribology Conference (AUSTRIB '02)*, Western Australia.

8. Bogy, D., Wu, L., Zeng, Q-H and Zhu, H., 1999, "Air Bearing Designs for 100 Gbit/in^2", TRIB-Vol. 9, *Proceedings of the Symposium on Interface Technology Towards 100 Gbit/in^2*, ASME, pp. 11-16

9. Bogy, D., Fong, W., Thornton, B., Zhu, H., Gross, H. and Bhatia, C., 2002, "Some Tribology and Mechanics Issues for 100 Gbit/in^2 HDD", *Intermag 2002 Conference*, Amsterdam, The Netherlands.

10. O'Hara, M., 1997, "Optimization of Hard Disk Drive Components", Ph.D. Thesis, University of California at Berkeley.

11. O'Hara, M. and Bogy, D., 1997, "The CML Air Bearing Optimization Program Version 1.5", Technical Report, Computer Mechanics Laboratory, University of California at Berkeley.

12. Jones, D. R., Perttunen, C. D. and Stuckman, B. E., 1993, "Lipschitzian Optimization Without the Lipschitz Constant ", *Journal of Optimization Theory and Application*, Vol. 79, No. 1, pp. 157-181.

13. Gablonsky, J. M., 1998, "An Implementation of the DIRECT algorithm", Technical Report CRSC-TR98-29, Center for Research in Scientific Computation, North Carolina State University.

14. Gablonsky, J. M. and Kelley, C. T., 2000, "A locally-biased form of the DIRECT algorithm", Technical Report CRSC-TR00-31, Center for Research in Scientific Computation, North Carolina State University.

15. Gablonsky, J. M., 2001, "DIRECT Version 2.0 User Guide", Technical Report CRSC-TR01-08, Center for Research in Scientific Computation, North Carolina State University.

	Initial ABS design			Optimized ABS design		
	OD	**MD**	**ID**	**OD**	**MD**	**ID**
FH (nm)	4.74	5.38	5.31	3.21	3.44	3.42
Roll (μrad)	1.52	1.34	-1.10	1.13	1.84	-1.46
Pitch (μrad)	98.3	99.2	98.5	88.9	90.2	90.5

Table 1 Summary of the optimization results for the 4-D case

	Initial ABS design			Optimized ABS design		
	OD	**MD**	**ID**	**OD**	**MD**	**ID**
FH (nm)	4.74	5.38	5.31	3.38	3.57	3.49
Roll (μrad)	1.52	1.34	-1.10	0.82	1.75	-1.56
Pitch (μrad)	98.3	99.2	98.5	90.9	92.3	91.9

Table 2 Summary of the optimization results for the 2-D case

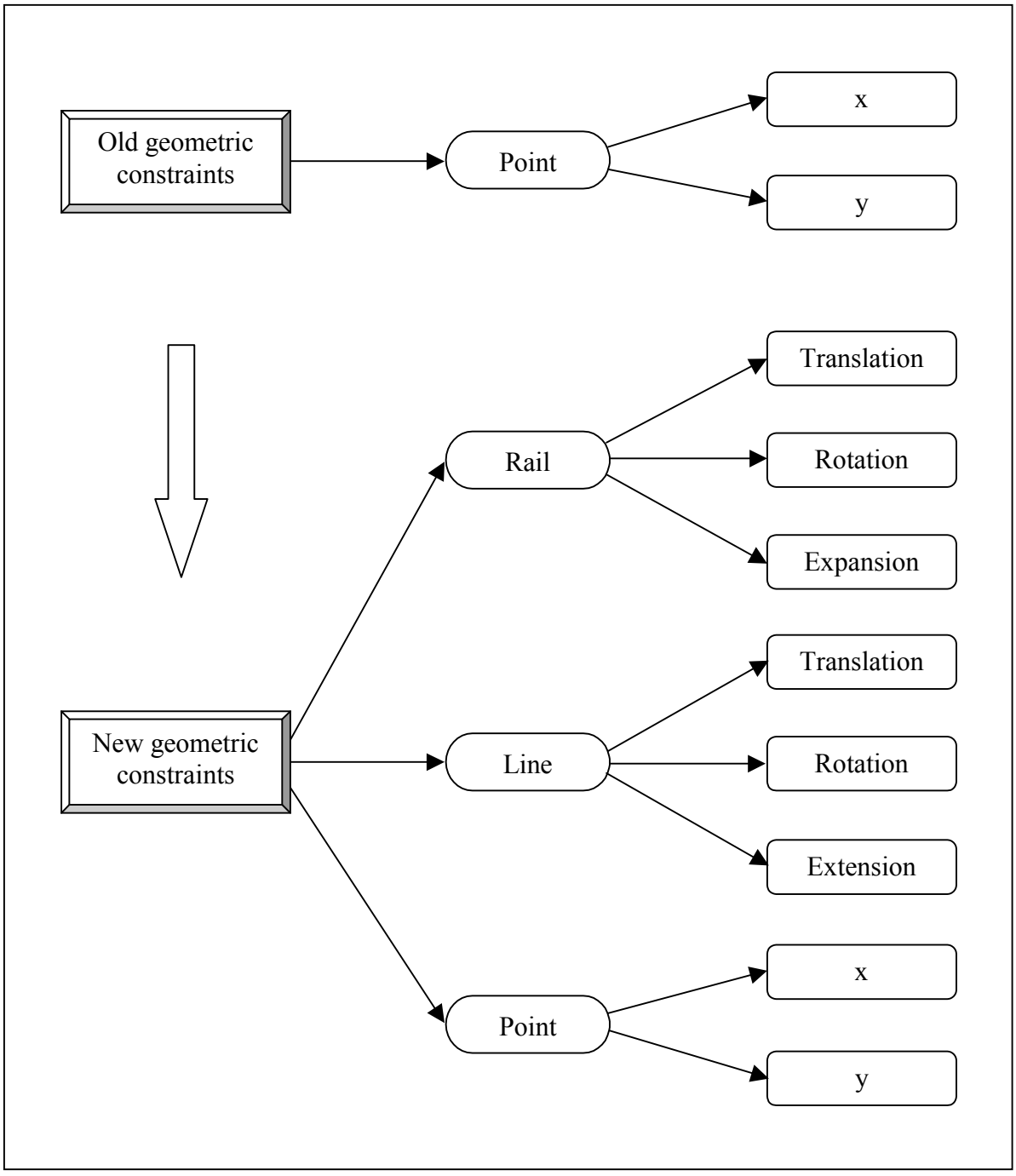

Fig. 1 Comparison between the old and the new geometric constraints

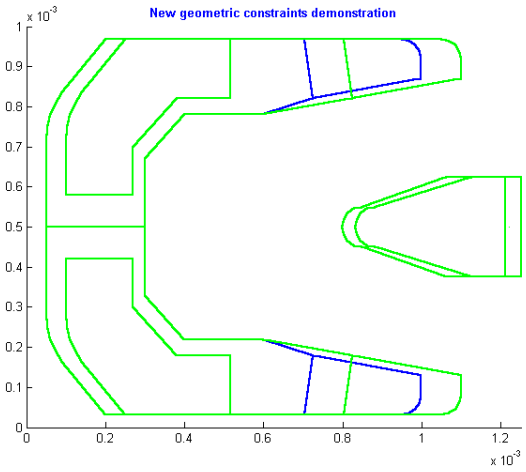

Fig. 2 Rail translation

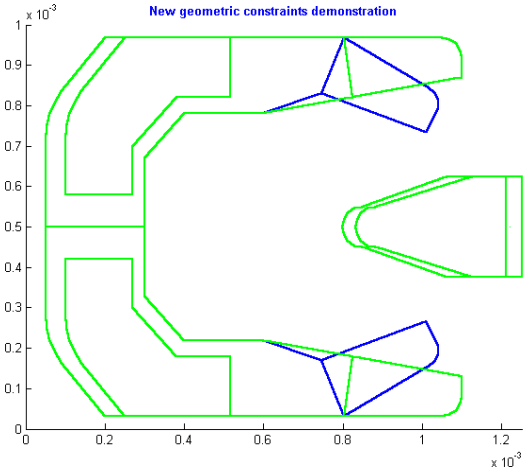

Fig. 3 Rail rotation

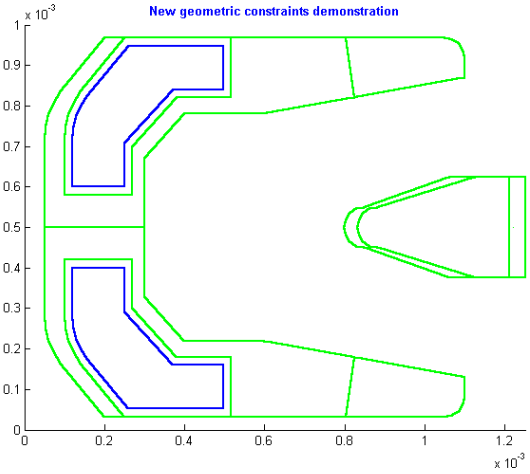

Fig. 4 Rail expansion

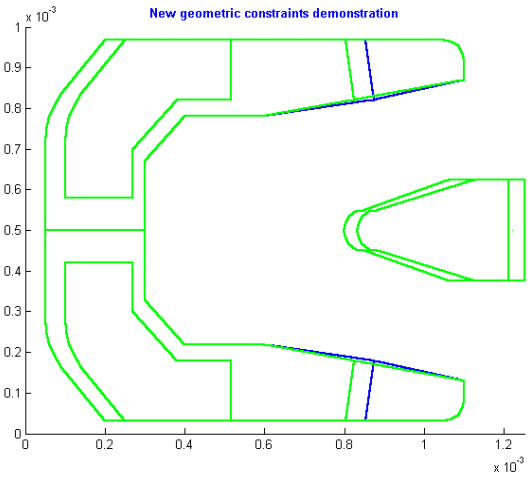

Fig. 5 Line translation

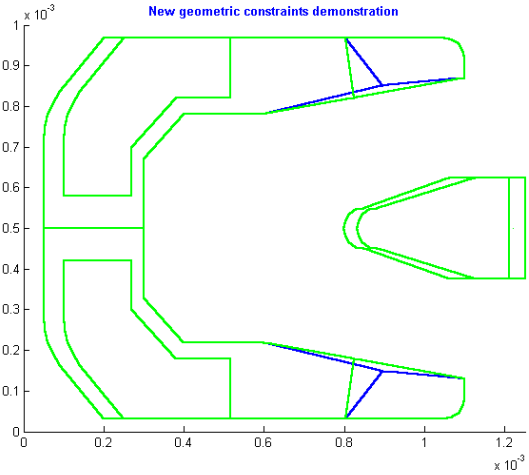

Fig. 6 Line rotation

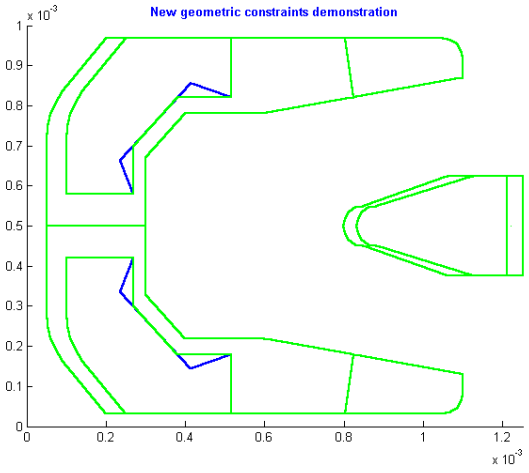

Fig. 7 Line extension

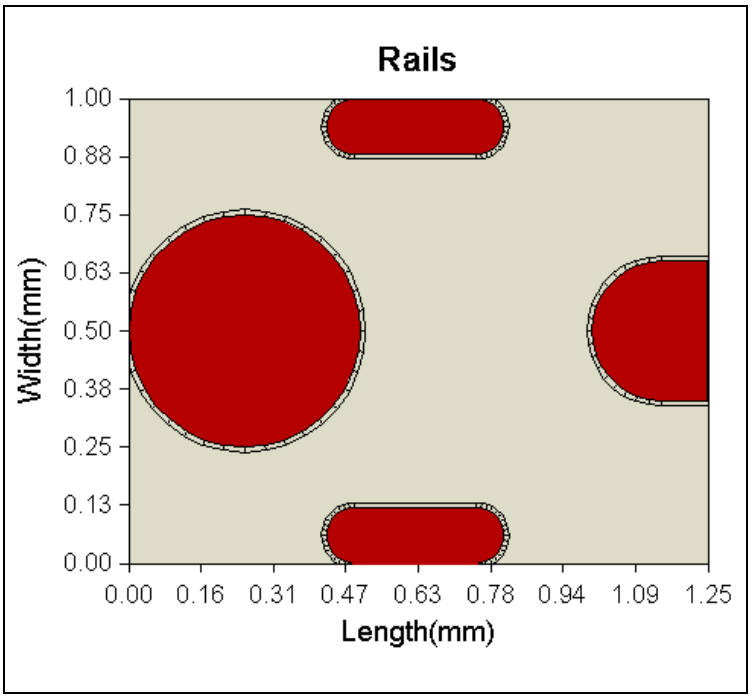

Fig. 8 Rail shape of the initial “Enterprise” slider design

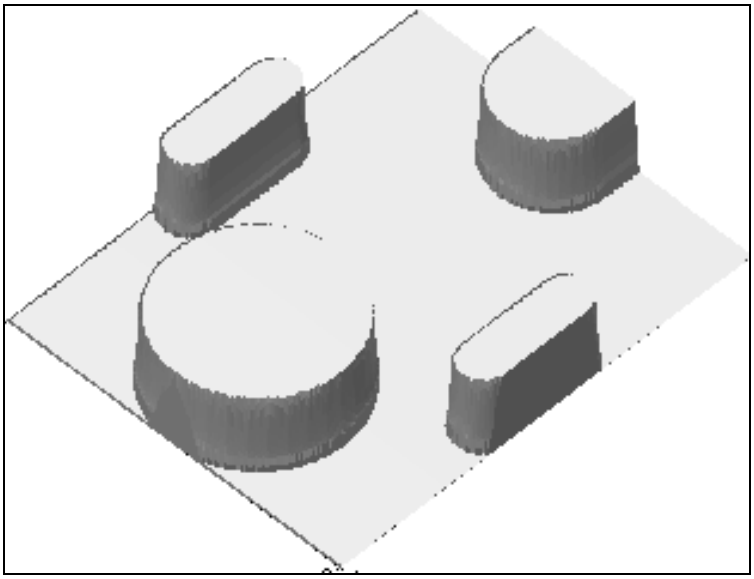

Fig. 9 3-D rail shape of the initial “Enterprise” slider design

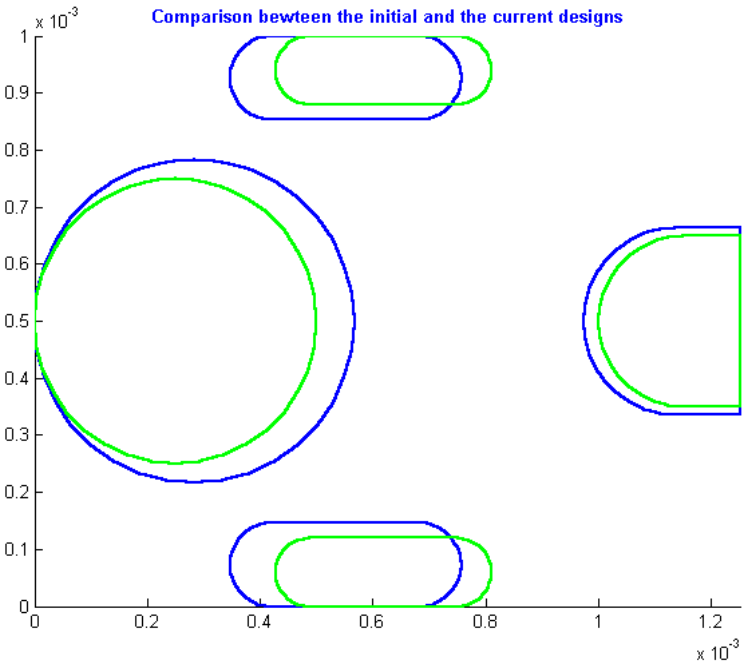

Fig. 10 Demonstration of the constraint rails prescribed for the 4-D case

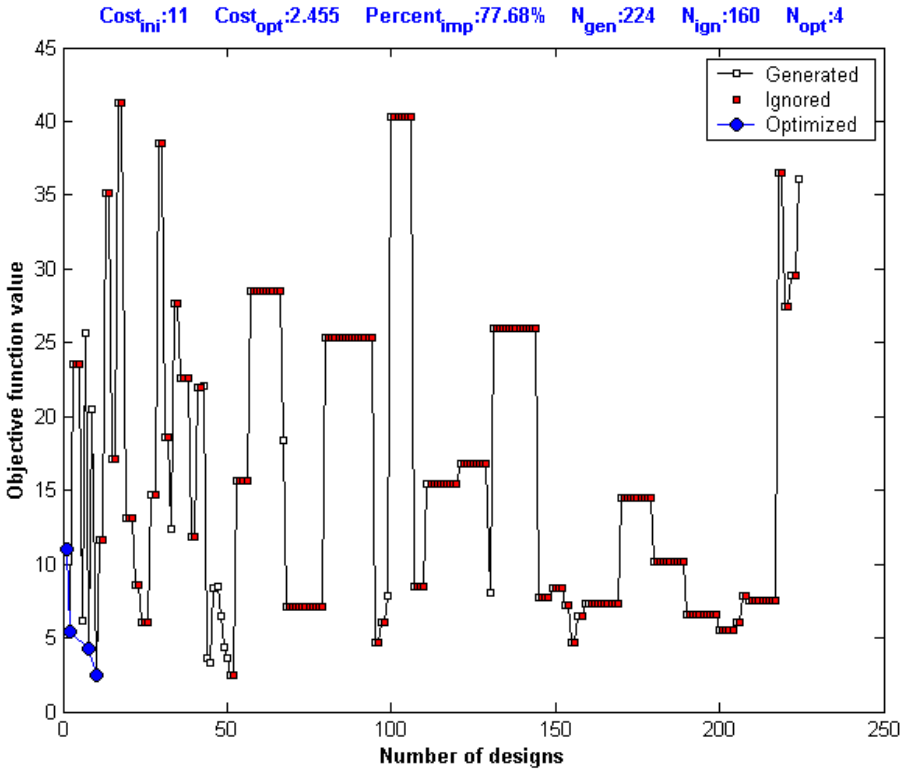

Fig. 11 Variation of the objective function value for the 4-D case

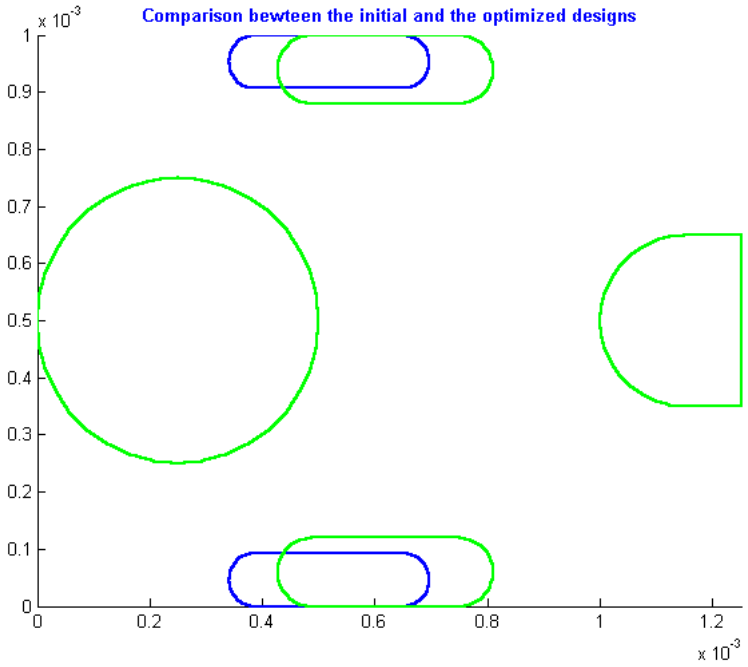

Fig. 12 Comparison between the initial design and the optimized design for the 4-D case

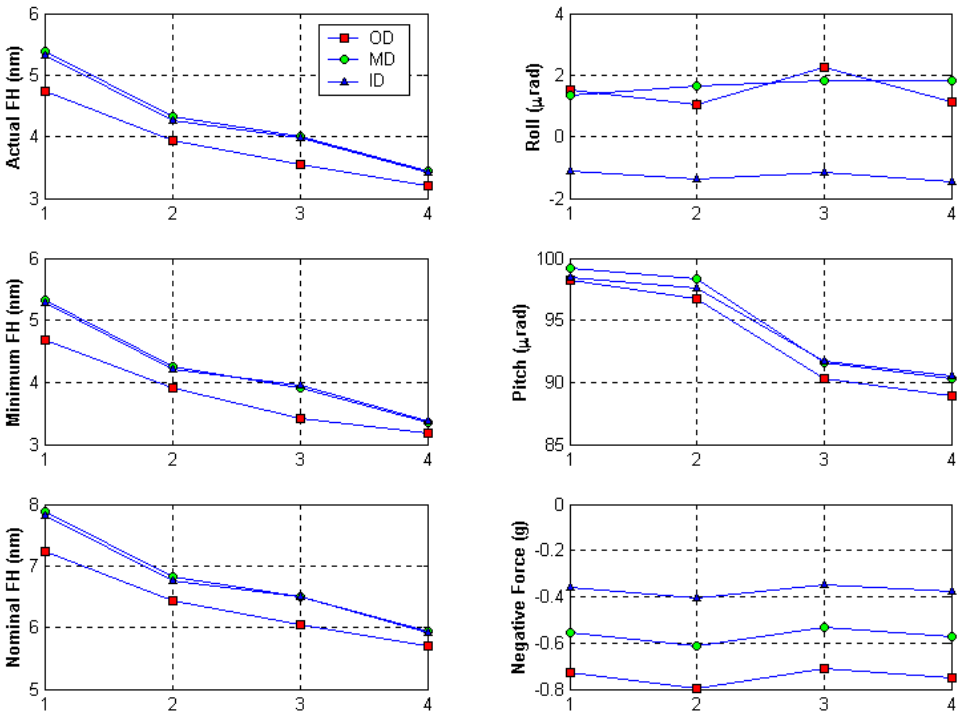

Fig. 13 Variations of the slider performance parameters for the 4-D case

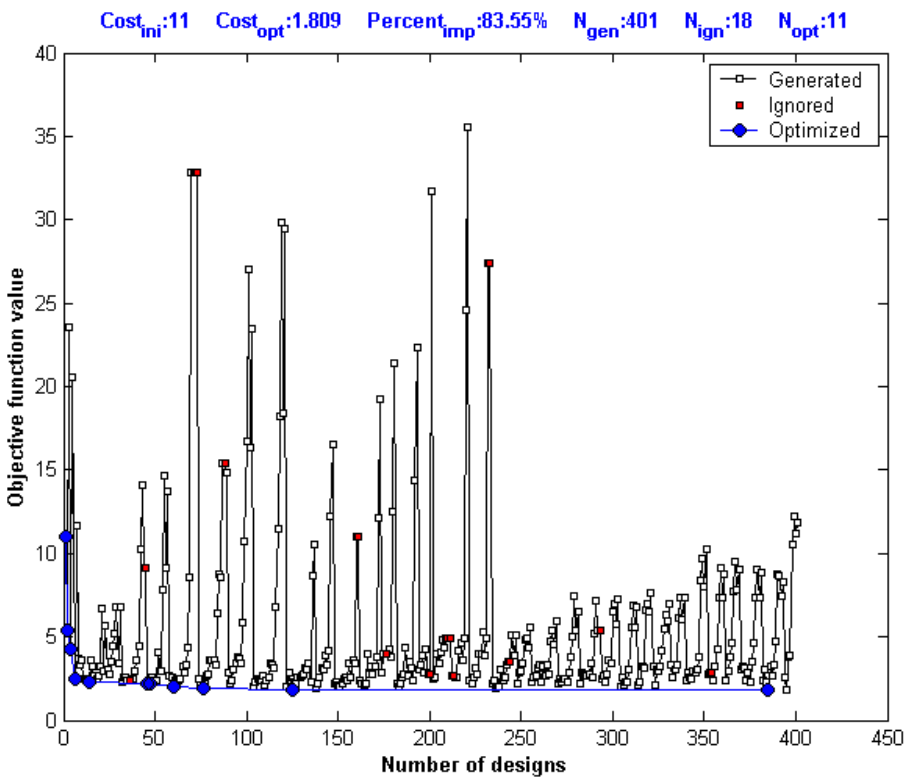

Fig. 14 Variation of the objective function value for the 2-D case

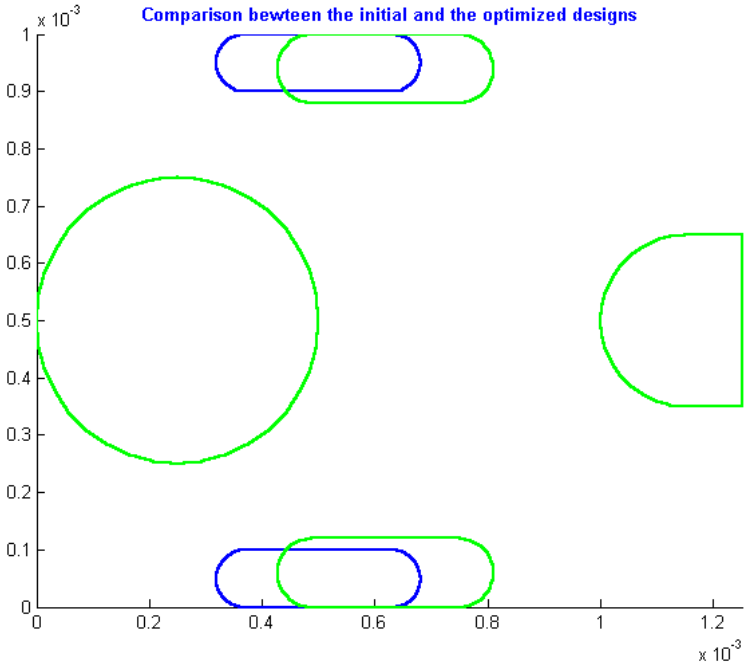

Fig. 15 Comparison between the initial design and the optimized design for the 2-D case

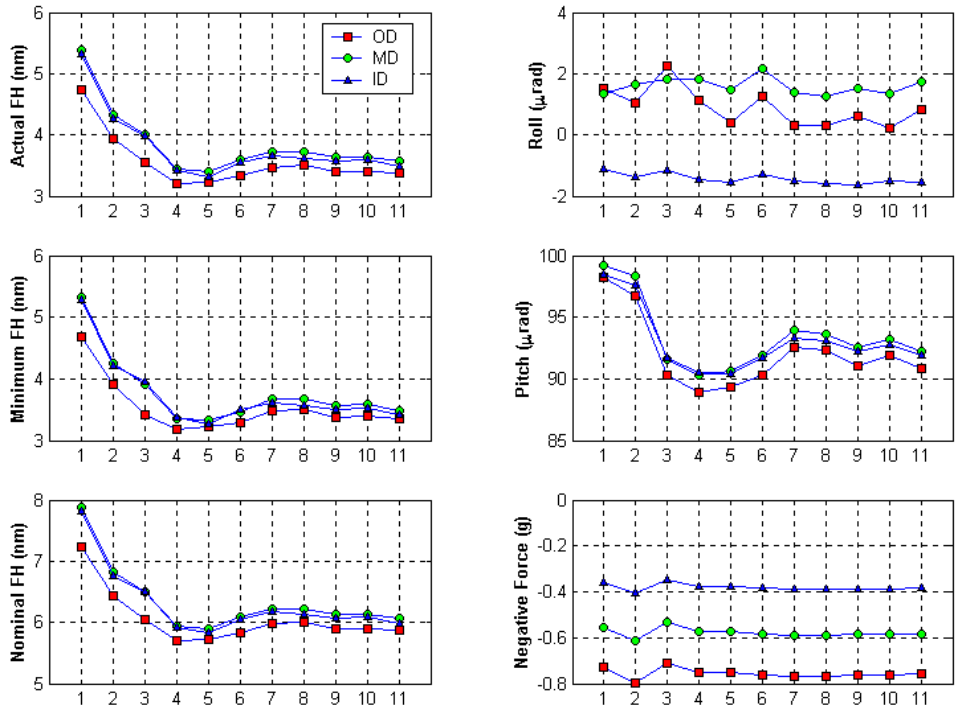

Fig. 16 Variations of the slider performance parameters for the 2-D case

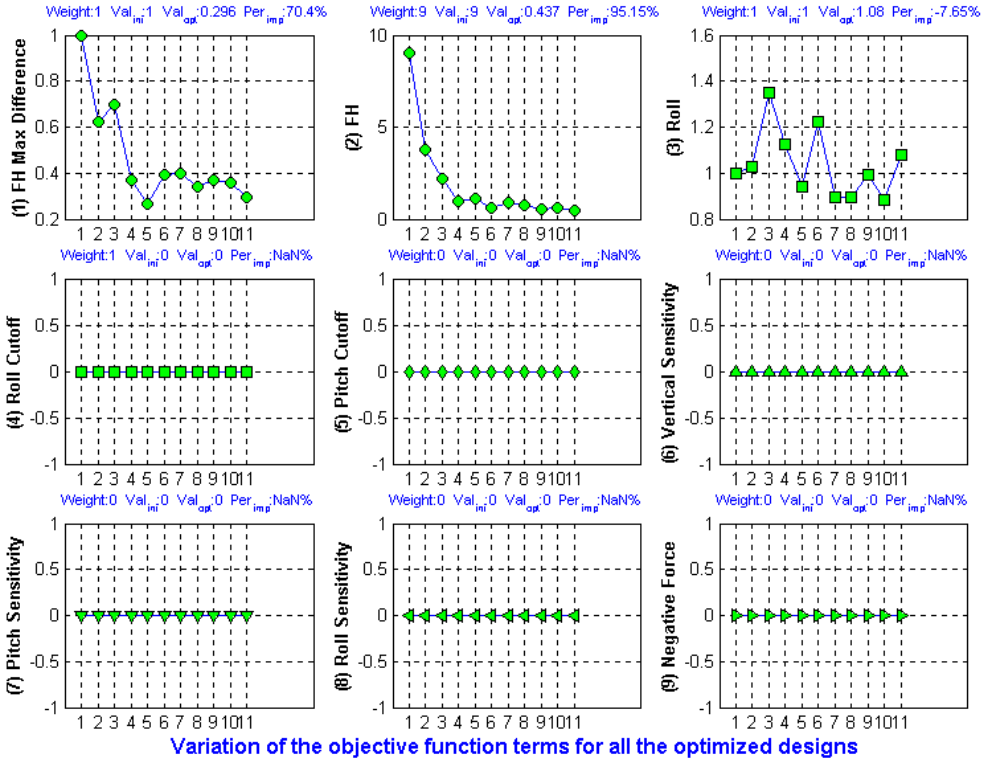

Fig. 17 Variations of the objective function terms for the 2-D case

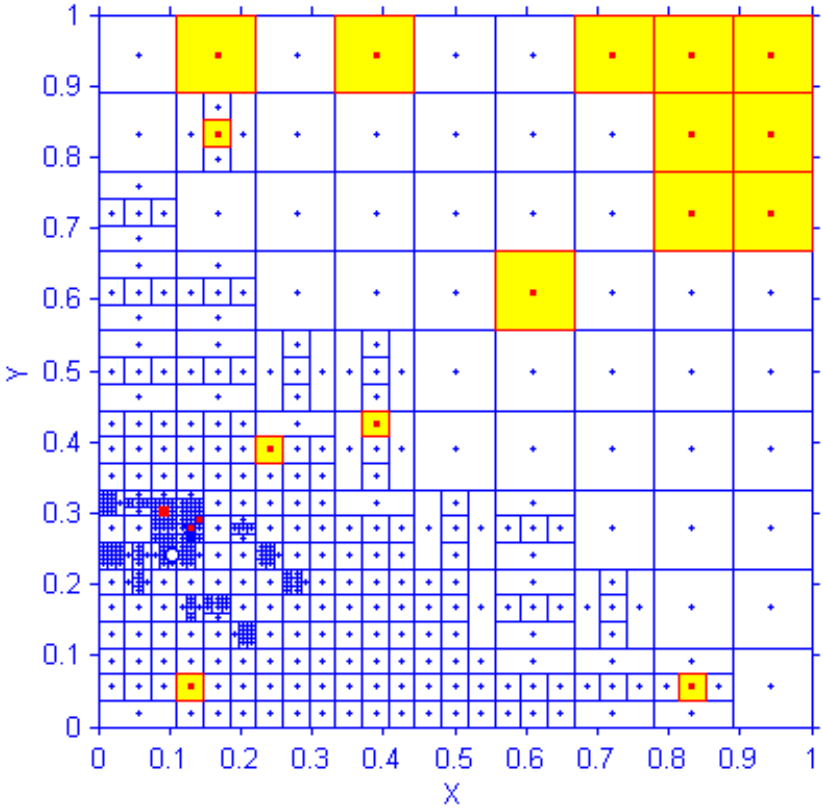

Fig. 18 Optimization results for the 2-D case

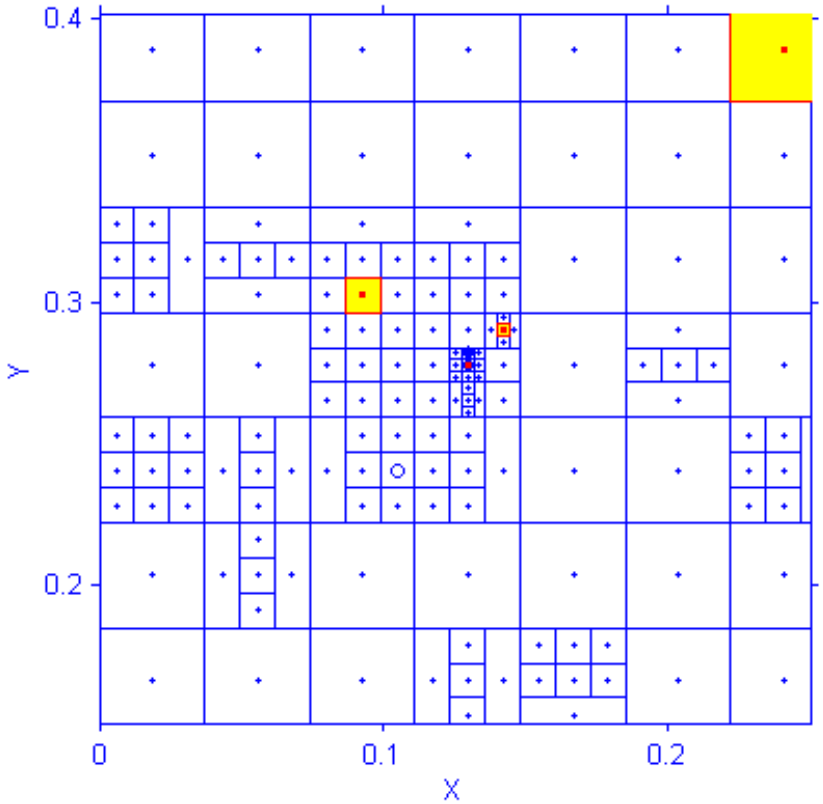

Fig. 19 Local zoom-in around the best point

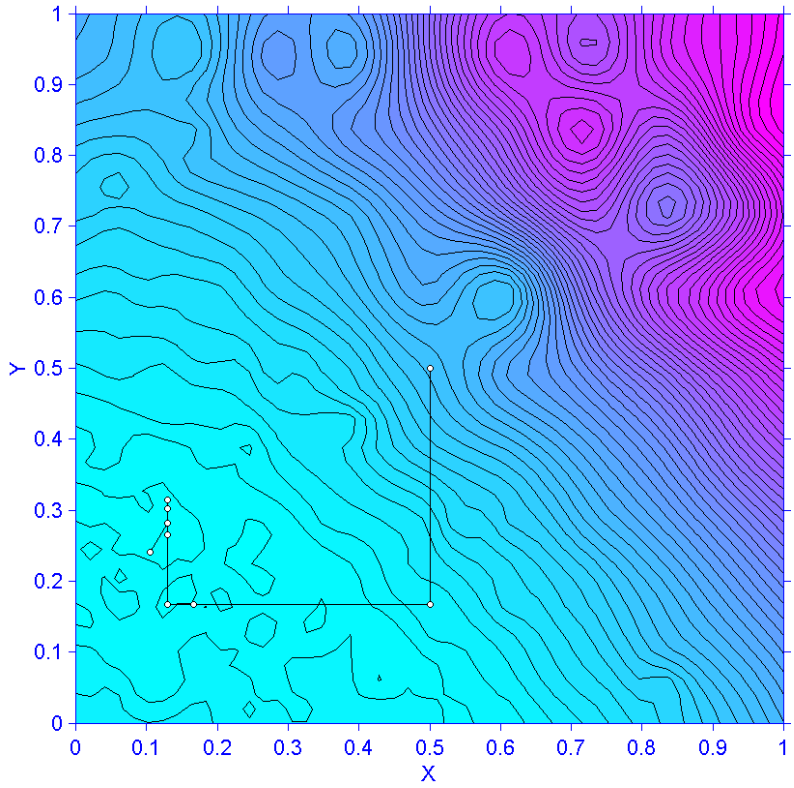

Fig. 20 Contour lines in the search space for the 2-D case

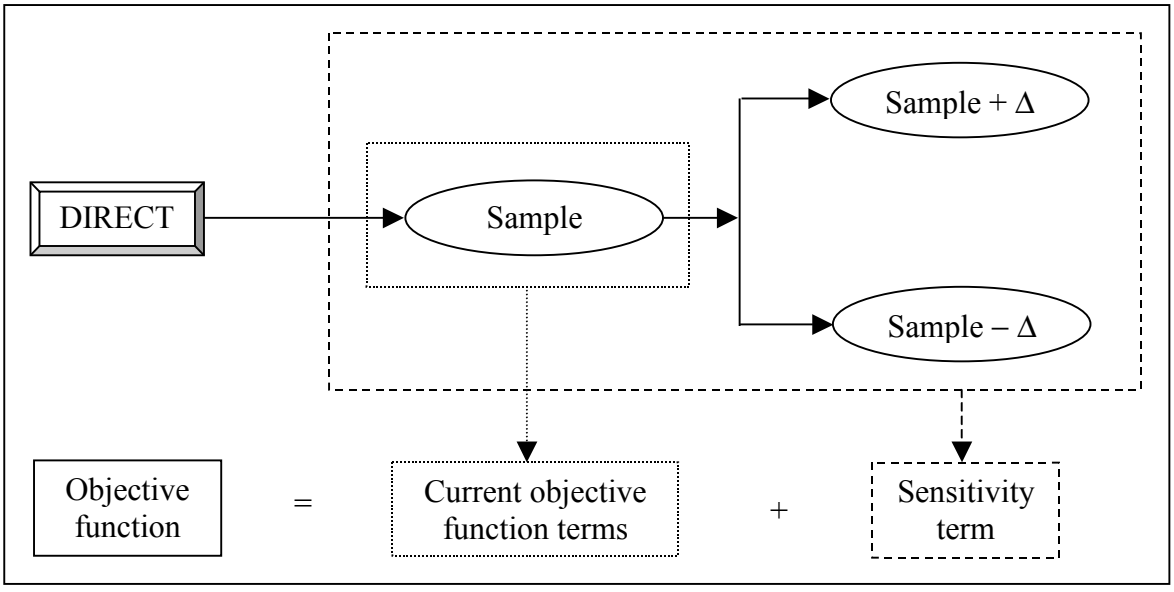

Fig. 21 Illustration of the sensitivity optimization process

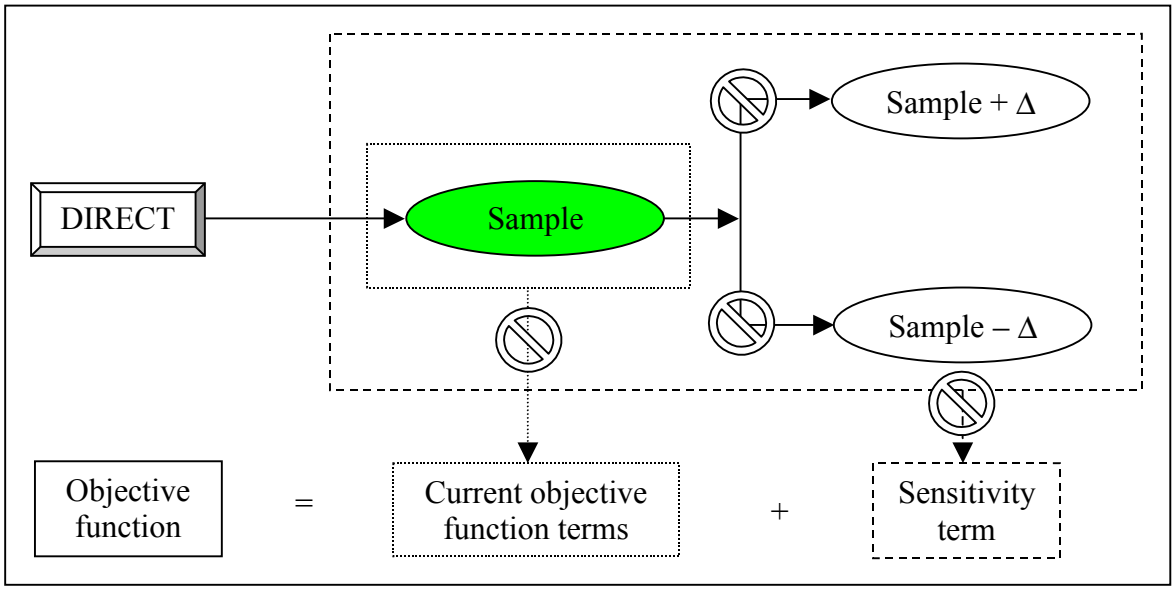

Fig. 22 Ways to improve the efficiency: Hidden constraints (1)

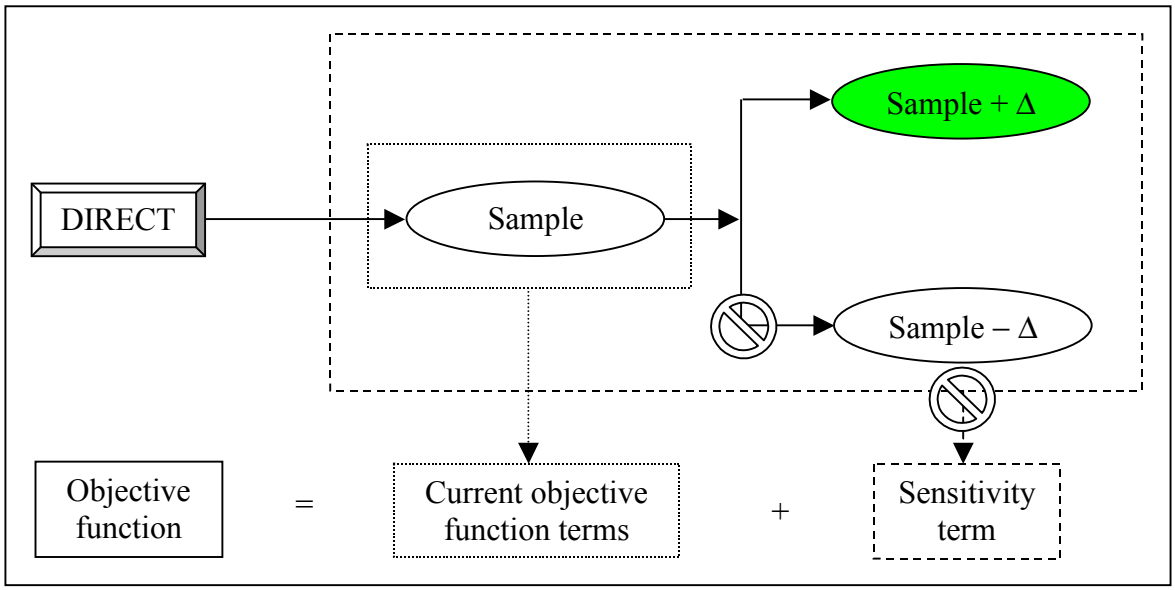

Fig. 23 Ways to improve the efficiency: Hidden constraints (2)

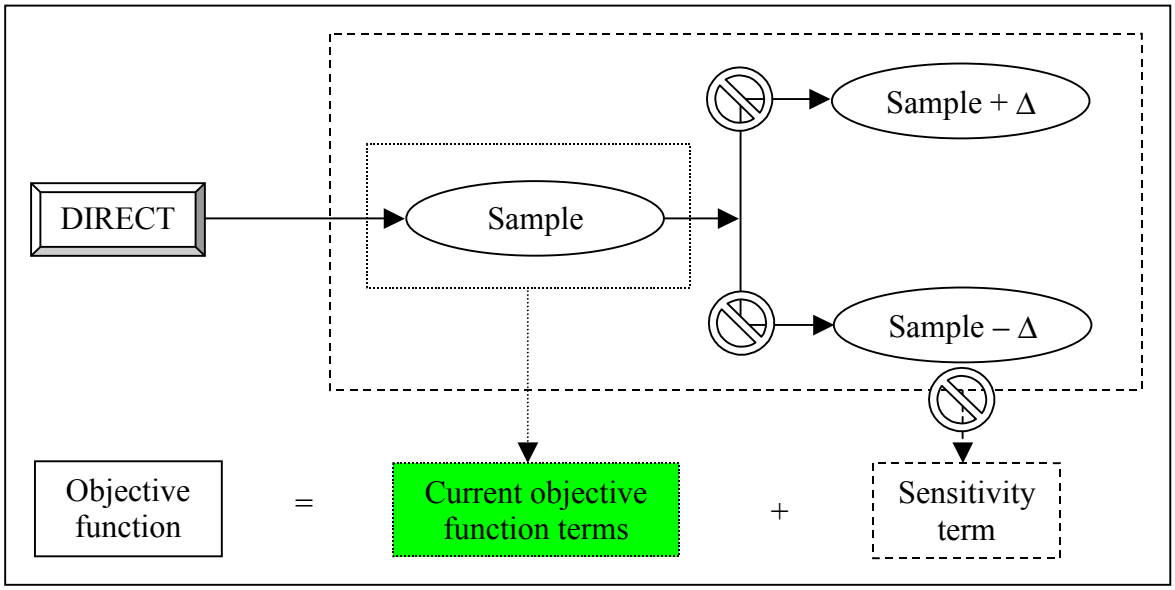

Fig. 24 Ways to improve the efficiency: First part of the objective function